1-1-2018

# Molecular Quantum Dot Cellular Automata Based on Diboryl Monoradical Anions

Xingyong Wang
*University of Wollongong*, xingyong@uow.edu.au

Lirong Yu
*Lanzhou University*

Venkatasaisandeep Inakollu
*University of Wollongong*, vi244@uowmail.edu.au

Xiaobo Pan
*Nanjing University, Lanzhou University*

Jing Ma
*Nanjing University*

*See next page for additional authors*

# Molecular Quantum Dot Cellular Automata Based on Diboryl Monoradical Anions


## Abstract

Field-effect transistor (FET)-based microelectronics is approaching its size limit due to unacceptable power dissipation and short-channel effects. Molecular quantum dot cellular automata (MQCA) is a promising transistorless paradigm that encodes binary information with bistable charge configurations instead of currents and voltages. However, it still remains a challenge to find appropriate candidate molecules for MQCA operation. Inspired by recent progress in boron radical chemistry, we theoretically predicted a series of new MQCA candidates built from diboryl monoradical anions. The unpaired electron resides mainly on one boron center and can be shifted to the other by an electrostatic stimulus, forming bistable charge configurations required by MQCA. By investigating various bridge units with different substitutions (ortho-, meta-, and para-), we suggested several candidate molecules that have potential MQCA applications.



## Disciplines

Medicine and Health Sciences

## Publication Details

Wang, X., Yu, L., Inakollu, V., Pan, X., Ma, J. & Yu, H. (2018). Molecular Quantum Dot Cellular Automata Based on Diboryl Monoradical Anions. The Journal of Physical Chemistry C: Energy Conversion and Storage, Optical and Electronic Devices, Interfaces, Nanomaterials, and Hard Matter, 122 (4), 2454-2460.



## Authors

Xingyong Wang, Lirong Yu, Venkatasaisandeep Inakollu, Xiaobo Pan, Jing Ma, and Haibo Yu

# Molecular Quantum-Dot Cellular Automata Based on Diboryl Monoradical Anions

Xingyong Wang,[1,2] Lirong Yu,[3] V. S. Sandeep Inakollu,[1] Xiaobo Pan*,[3] Jing Ma*,[4] Haibo Yu*[1,2]

[1]School of Chemistry, University of Wollongong, NSW 2522, Australia

[2]Illawarra Health and Medical Research Institute, Wollongong, NSW 2522, Australia

[3]College of Chemistry and Chemical Engineering, Lanzhou University, 222 Tianshui South Road, Lanzhou 730000, P. R. China

[4]School of Chemistry and Chemical Engineering, Institute of Theoretical and Computational Chemistry, Key Laboratory of Mesoscopic Chemistry of MOE, Nanjing University, Nanjing 210093, P. R. China

**ABSTRACT:** The field-effect transistor (FET) based microelectronics is approaching its size limit due to unacceptable power dissipation and short-channel effects. Molecular quantum-dot cellular automata (MQCA) is a promising transistorless paradigm, which encodes binary information with bistable charge configurations instead of currents and voltages. However, it still remains a challenge to find appropriate candidate molecules for MQCA operation. Inspired by recent progress in boron radical chemistry, we theoretically predicted a series of new MQCA candidates built from diboryl monoradical anions. The unpaired electron resides mainly on one boron center and can be shifted to the other by an electrostatic stimulus, forming bistable charge configurations required by MQCA. By investigating various bridge units with different substitutions (*ortho*-, *meta*-, and *para*-), we suggested several candidate molecules that are potential in MQCA applications.

## 1. INTRODUCTION

When shrinking the size close to its quantum limit, the field-effect transistor (FET) based electronic devices will face a significant performance degradation as a result of the unacceptable power dissipation and short-channel effects.[1] As a promising alternative approach, quantum-dot cellular automata (QCA) has attracted considerable attentions for building the next-generation microelectronic elements.[2-3] In QCA, binary information is represented by the charge configuration of a cell with four dots and two charges. The two charges favor a diagonal arrangement due to Coulomb repulsion, forming the bistable states that can be used to encode logic "0" and "1" (Scheme 1a). The binary signal transmission can be realized via intercellular Coulomb coupling with no current flow, thus resulting in extremely low power dissipation.[4] The first successful QCA was based on metal islands scaling at 60 nm, but only worked at cryogenic temperatures (below 100 mK).[1,5] One solution to achieve room temperature operation is using magnetic metals[6-7] or silicon atom dangling bonds[8] to make the dots. The other way is decreasing the size of the device and molecular-sized QCA is expected to work at room temperature, making molecular QCA (MQCA) an attractive target.[9-12] In the MQCA architecture, a single molecule usually contains two "dots" and can be viewed as a half-cell, thus there are two ways to construct a MQCA wire: side-by-side or head-to-tail (Scheme 1b).[9] Signal transmission in MQCA occurs thanks to intermolecular Coulomb interaction, due to a neighboring molecule, alters the charge configuration of another molecule in a nonlinear way. In practice, it is not an easy task to find appropriate molecules that can be utilized in MQCA. The key requirement is that the candidate molecule needs to bear bistable charge configurations that can be switched by Coulomb interactions.[13-15] During the last two decades, a variety of candidate systems have been proposed, including mixed-valence organometallic complexes,[16-33] mixed-spin grid complexes,[34] metal cluster carboxylates,[35] zwitterionic boron−allyl complexes,[36-37] and double-cage fluorinated fullerene anions.[38-39] It is still a challenge to put them to practical applications due to difficulties in synthesis or surface attachment.

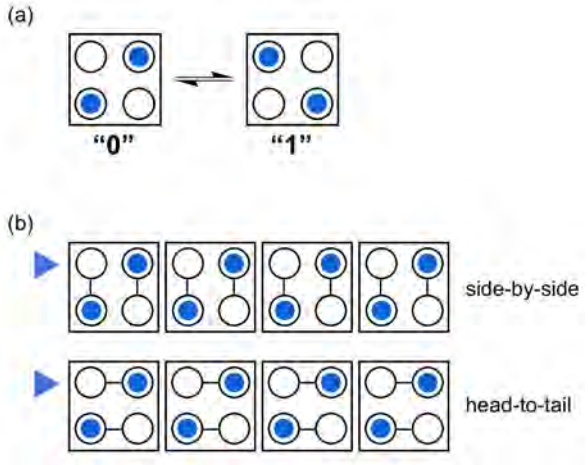


**Scheme 1.** (a) Schematic of QCA cells with two bistable states encoding logic "0" and "1"; (b) Two types of MQCA wires. The solid triangle represents the electrostatic driver.

Owing to the inherent electron deficiency, boron-centered radicals can be readily formed, which are good charge containers and may serve as the "dots" in MQCA. The diradical dianion of a diboryl compound **1-Mes** (2,2"-bis(dimesitylboranyl)-1,1':4',1"-terphenyl) was recently observed by electron paramagnetic resonance (EPR) measurements.[40] Based on such kind of π-conjugated spacer linked diboryl structure, herein we proposed a new MQCA candidate system − diboryl monoradical anions, in which the charge was mainly localized on one boron atom and can be switched upon an electrostatic stimulus. We focus on the theoretical exploration of the eligibility of such kind of diboryl monoradical anions (e.g. **1-Mes**$^{\bullet-}$) as MQCA candidates. Spin density distribution (Figure 1b) and the singly occupied molecular orbital (SOMO, Figure 1c) obtained from density functional theory (DFT) calculations show that the unpaired electron in **1-Mes**$^{\bullet-}$ is primarily localized on one boron atom (60%), with 25% on the carbon atoms of the adjacent benzene moiety and negligible distribution on the central benzene unit. Analogous to the previous works,[20, 38] the spin densities and Mulliken charges of the two boron atoms were chosen to characterize the charge configuration. In this work, it will be demonstrated that the unpaired electron can shift between the two boron centers upon an external electrostatic perturbation and form bistable charge configurations. Based on this framework, a series of analogous candidates with different spacers and substitutions have been investigated and a design strategy has been proposed.

As a class of conjugated organoborane, the neutral *para*-substituted diboryl compounds with various π-linkers studied in this work may have potential applications in optoelectronics, such as organic light-emitting diodes (OLEDs), organic field-effect transistors (OFETs) and photovoltaic devices,[41,42] due to the overlap of empty p-orbital on boron with the π*-orbitals of the conjugated bridging moieties. They may also act as effective anion sensors owning to the electron deficiency in the boron atom.[43]

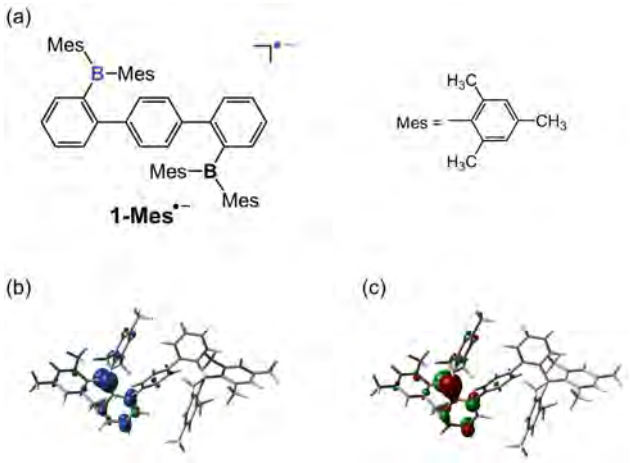


**Figure 1.** (a) Chemical structure, (b) spin density distribution and (c) SOMO of **1-Mes**$^{\bullet-}$. Spin densities and SOMO were calculated at UCAM-B3LYP/6-31G(d) and drawn at the isovalue of 0.005 e/Bohr$^3$ and 0.05 (e/Bohr$^3$)$^{1/2}$, respectively.

## 2. COMPUTATIONAL DETAILS

All geometry optimizations and single point energy calculations were carried out at the (U)CAM-B3LYP/6-31G(d) level of theory, which has been proved to be robust in describing the electronic structures of diboryl compounds.[40] Vibrational frequency calculations were carried out to confirm that all optimized geometries correspond to energy minima. The energy of the lowest unoccupied molecular orbital (LUMO) for **1** was evaluated at the B3LYP/6-311+G(d,p) level, which proves to perform well in predicting the half-wave reduction potential for arylborane compounds in experimental cyclic voltammogram measurements.[44] An electric dipole field was applied along the axis connecting the two boron atoms (B1 and B2) to model the external electric field. The electrostatic driver was modeled with a unit point charge. The dipole moment was calculated using molecular center of mass as the origin. The spin density distributions and SOMOs were drawn at the isovalue of 0.005 *e*/Bohr$^3$ and 0.05 (*e*/Bohr$^3$)$^{1/2}$, respectively. No constraint was exerted when doing geometry optimizations in the presence of an electric field. All calculations were performed with the Gaussian 09 program package.[45]

## 3. RESULTS AND DISCUSSION

### 3.1. Simplification of the Model: Replacing Mes with Ph.

In compound **1-Mes**$^{\bullet-}$, the 2,4,6-trimethylphenyl (Mes) substituents around the boron centers are rather bulky (Figure 1a). By comparing the electronic structures of **1-Mes**$^{\bullet-}$ and its phenyl (Ph) derivative **1**$^{\bullet-}$, we

find that replacing the Mes substituent with phenyl group resulted in similar charge localization property. As shown in Table 1, for both compounds the spin density mainly resides on B1 with significantly low population on B2. The Mulliken charge displays a consistent scenario, where B1 is negatively charged while B2 bears a nearly zero charge. Both **1-Mes**$^{\bullet-}$ and **1**$^{\bullet-}$ have a large dipole moment, which is in line with the highly localized charge distribution. Comparing the data in Table 1, we can see the differences in spin densities are only 0.037 and 0.025 for B1 and B2, respectively. The Mulliken charges differ within 0.01 and the dipole moments are identical. Therefore, to save computational cost, we based our study on such model compounds with phenyl group as the substituent.

**Table 1.** Spin densities ($\mathbf{S}_{B1}$, $\mathbf{S}_{B2}$)[a], Mulliken charges ($\mathbf{Q}_{B1}$, $\mathbf{Q}_{B2}$) and dipole moments ($\boldsymbol{\mu}_x$, in Debye[b]) of **1-Mes**$^{\bullet-}$ and **1**$^{\bullet-}$.

| | $\mathbf{S}_{B1}$ | $\mathbf{S}_{B2}$ | $\mathbf{Q}_{B1}$ | $\mathbf{Q}_{B2}$ | $\boldsymbol{\mu}_x$ |
|---|---|---|---|---|---|
| **1-Mes**$^{\bullet-}$ | 0.604 | 0.018 | –0.218 | –0.027 | 13.0 |
| **1**$^{\bullet-}$ | 0.567 | 0.043 | –0.209 | –0.022 | 13.0 |

[a]B1 and B2 represent the two boron atoms. [b]The *x* direction corresponds to the axis that connects B1 and B2.

For the sake of experimentalists following this work, the half-wave reduction potential ($E_{1/2}^{Red}$) of the non-radical neutral compound **1**, as well as the energy for disproportionation ($E_d$) of monoradical **1**$^{\bullet-}$ to neutral **1** and diradical dianion [**1**$^{\bullet\bullet}$]$^{2-}$, were investigated prior to exploring the QCA properties of **1**$^{\bullet-}$. The reduction potential $E_{1/2}^{Red}$ was estimated to be –2.71 V vs FcH/FcH$^+$ based on **1**'s LUMO energy level (see SI for calculation details), indicating that **1**$^{\bullet-}$ is potentially accessible via reduction of **1**. The disproportionation energy ($E_d$ = 42.0 kcal/mol) calculated in the gas phase implies the disproportionation from the monoradical form to the neutral and dianionic species is not energetically favored. Therefore, we expect that the synthesis of such diboryl monoradical compound should be experimentally feasible.

### 3.2. Electric Field Induced Bistable Charge Configurations Transformation

To achieve the switch between logic "0" and "1" states, the charge should be able to shift between the MQCA "dots" driven by Coulomb interactions. By applying an external electric dipole field ($\boldsymbol{E}$) with increasing intensities on **1**$^{\bullet-}$, we observed an evident charge transfer from B1 to B2 when $\boldsymbol{E}$ was greater than 0.001 au. As shown in Table S1 and Figure 2, a weaker electric field ($\boldsymbol{E}$ = 0.0005 au) only causes a slight charge redistribution. However, when $\boldsymbol{E}$ rises from 0.0005 au to 0.0007 au, $\mathbf{S}_{B1}$ decreases dramatically while $\mathbf{S}_{B2}$ goes up significantly. The Mulliken charges show the same trend. The dipole moment flips to the

opposite direction with a similar magnitude. When ***E*** increases further to 0.002 au, the changes become less pronounced. It is worth mentioning that all these data were obtained based on single point energy calculations on the same geometry, i.e., the optimized geometry of $\mathbf{1}^{\bullet-}$ in the absence of an electric field, indicating that $\mathbf{1}^{\bullet-}$ is highly polarizable and this intramolecular charge transfer can happen without significant geometric changes. To investigate the influence of the electric field on the molecular structure of $\mathbf{1}^{\bullet-}$, geometry optimizations under ***E*** intensities of 0.001, 0.0015 and 0.002 au were performed, resulting in nearly identical structures with all atom positional root-mean-square deviations (RMSDs) < 0.04 Å (Figure S1). Then the field was removed and a subsequent geometry optimization, which can be regarded as a "relaxation" process, led to the counterpart of $\mathbf{1}^{\bullet-}$, named $\mathbf{1}^{\bullet-}$'. Bearing the same energies, but inversed spin densities, dipole moments and bonding conditions, $\mathbf{1}^{\bullet-}$ and $\mathbf{1}^{\bullet-}$' formed bistable charge configurations (Figures 3 and S2, Table S2) that can be switched by applying an external electric field.

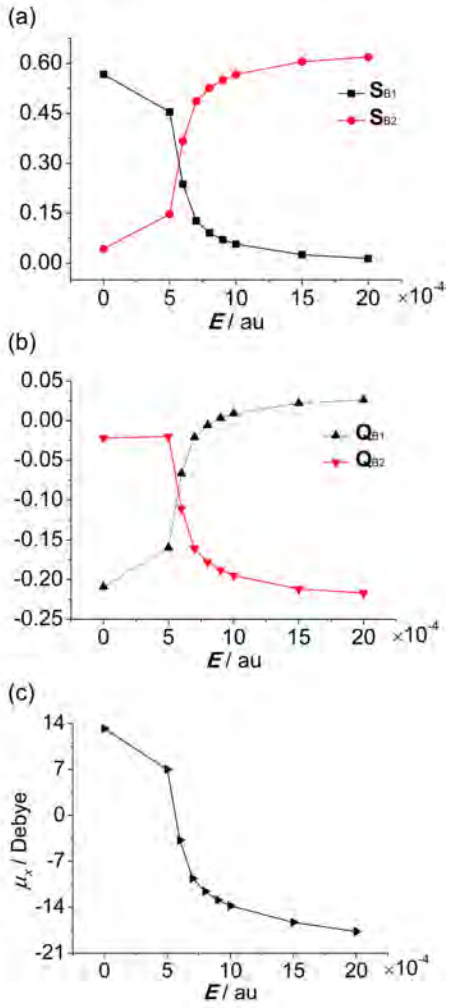


**Figure 2.** (a) Spin density, (b) Mulliken charge and (c) dipole moment of $\mathbf{1}^{\bullet-}$ under different electric field intensities.

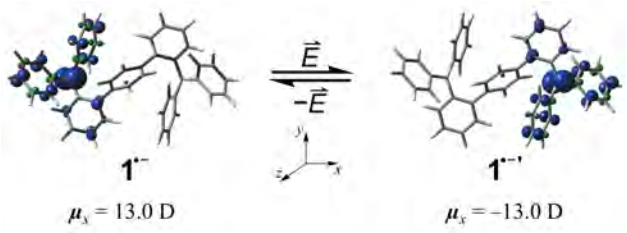


**Figure 3.** Bistable charge configurations formed via intramolecular charge transfer driven by an external electric field, displayed as the inversion of spin density and dipole moment (***E*** = 0.001 au).

### 3.3. Signal Transmission through MQCA

In order to determine whether the binary signal, which is represented as bistable charge configurations $\mathbf{1}^{\bullet-}$ and $\mathbf{1}^{\bullet-\prime}$, can be transmitted via intercellular Coulomb interactions, the response to an external driver has been investigated based on a dimer model with either side-by-side or head-to-tail arrangement (see Figure S3a and S3b for more details). The dimer model consists of two equivalent $\mathbf{1}^{\bullet-}$ molecules and only single point energy calculations were performed without geometry optimization due to large computational cost. According to the above results in **Section 3.2**, the intramolecular charge transfer can take place without geometric relaxation, which validates our model setup. The driver was modeled by a negative unit point charge ($q$ = –1.0e). The location of the driver and the intermolecular distance was chosen to guarantee sufficient Coulomb coupling between neighboring molecules without much unfavorable long range electrostatic interactions, while maintaining a roughly square geometry.[12]

Even without an external driver, the dimer in side-by-side arrangement displays a diagonal charge configuration (Figure S3c) due to Coulomb repulsion, which, in contrast, pushes the charges to the molecular edges in the head-to-tail array (Figure S3d). When a negatively charged driver was placed beside the dimer, the extra charge residing on the nearest boron center would be driven to the other boron center, which subsequently induced the charge transfer of the neighboring molecule (Figure 4). And adjusting the position of the driver would achieve either “0” to “1” or “1” to “0” logic level conversion (Figures 4 and S4). The transmission of information maintained when the charge of the driver was reduced from –1.0e to –0.5e. To further examine the state switching between two pairing four-dot cells, we replaced the driver with two point charges located in the position of two antipodal boron atoms to mimic the charge perturbation from a neighboring cell (Figure S5). The magnitude of charge ($q$ = –0.645e) was set as the sum of the Mulliken charge of the boron radical center along with the two phenol substituents (-$BPh_2$). A similar charge configuration switching was observed (Figure S5), demonstrating that binary signal control and information transmission can be fulfilled. The success of building MQCA with $\mathbf{1}^{\bullet-}$ inspires us to explore other candidates based on diboryl monoradical anions and in the following sections, we will focus on regiochemical effect and the influence of central bridge unit.

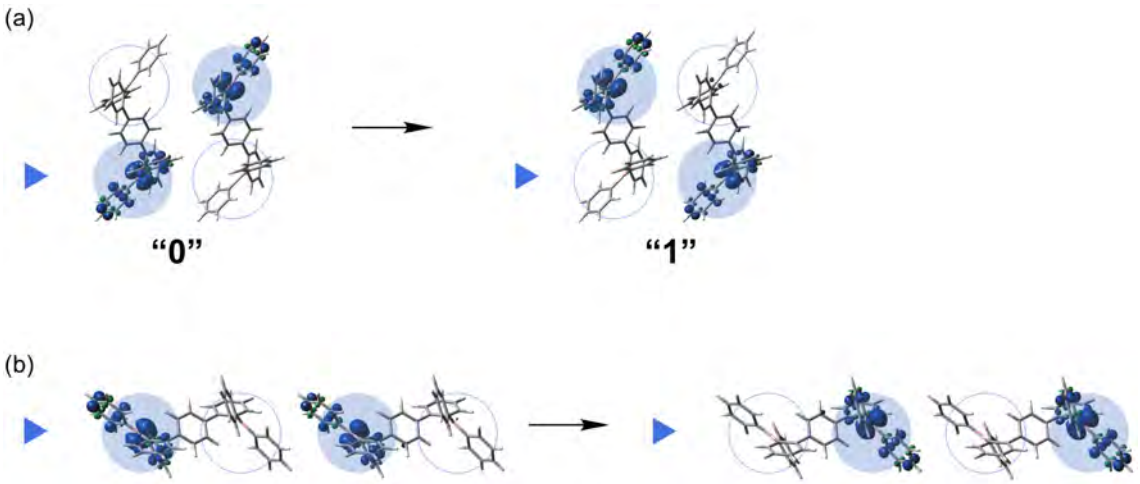


**Figure 4.** MQCA response to a point charge driver (the blue triangle) demonstrated by spin density redistributions. The translucent blue shades and circles are used to highlight "dots" in an MQCA cell.

### 3.4. Design of Other MQCA Candidates

#### 3.4.1. Bridge Effect

The electronic structure of spacer connected radical compounds has a bridge dependence.[46-48] It is interesting to probe the influence of bridge moiety on the performance of MQCA candidates. Adopting the *ortho*-substitution that is similar to $\mathbf{1}^{\bullet-}$, eight spacers were investigated, including oligophenyl, naphthyl, anthryl, (oligo)thiophene and ethynyl groups (Figure 5). After geometry optimization, again we examined the charge distribution properties that are shown in Table 2 and Figure 6, which display two distinct profiles. While $\mathbf{2}^{\bullet-}$, $\mathbf{3}^{\bullet-}$, $\mathbf{4}^{\bullet-}$ and $\mathbf{6}^{\bullet-}$ manifest similar properties to $\mathbf{1}^{\bullet-}$ with charge localized on one boron center and may serve as potential MQCA candidates, the rest exhibit symmetrical charge distributions, either mainly over the bridge ($\mathbf{5}^{\bullet-}$, $\mathbf{7}^{\bullet-}$, $\mathbf{8}^{\bullet-}$) or having a proportion evenly on two boron centers ($\mathbf{9}^{\bullet-}$). It is interesting that the switchover from dot-localized to bridge-localized behavior occurs in an all-or-nothing fashion. Going from phenyl to triphenyl bridge group (from $\mathbf{1}^{\bullet-}$ to $\mathbf{2}^{\bullet-}$ to $\mathbf{3}^{\bullet-}$), the charge localization maintains with increasing magnitude of dipole moment. However, when replacing the phenyl group to thiophene, only the monothiophene connected $\mathbf{6}^{\bullet-}$ exhibits localized charge. Although bearing similar spacers, $\mathbf{4}^{\bullet-}$ and $\mathbf{5}^{\bullet-}$ show considerably different properties. The isomer of $\mathbf{5}^{\bullet-}$ ($\mathbf{5'}^{\bullet-}$), in which the boron-$Ph_2$ groups were bonded to the two peripheral benzene rings of the anthracene bridge, shows similar spin density distribution (Figure S6). It appears that diboryl monoradicals with planar bridge units bearing larger conjugation extent, like the anthryl, bithiophene and trithiophene groups, favor a bridge-localized structure. By applying an external electric field upon the bridge-localized candidates ($\mathbf{5}^{\bullet-}$, $\mathbf{7}^{\bullet-}$, $\mathbf{8}^{\bullet-}$, $\mathbf{9}^{\bullet-}$) like we did for $\mathbf{1}^{\bullet-}$ in **Section 3.2**, we

found the symmetrical charge distribution changes gradually to a dot-localized pattern when the field intensity increases from 0.001 au to 0.002 au (Table S3), thus featuring potential MQCA candidates. This result indicates that a molecule with a zero or negligible dipole moment under field-free conditions may also function in an MQCA application, as long as its polarizability is sufficient to localize charge on one side of the molecule in response to an appropriate driving electric field. However, since a strong electric field (0.002 au) is required to achieve the charge localization state, such bridge-localized MQCA candidates are not the ideal choice compared to the naturally dot-localized ones.

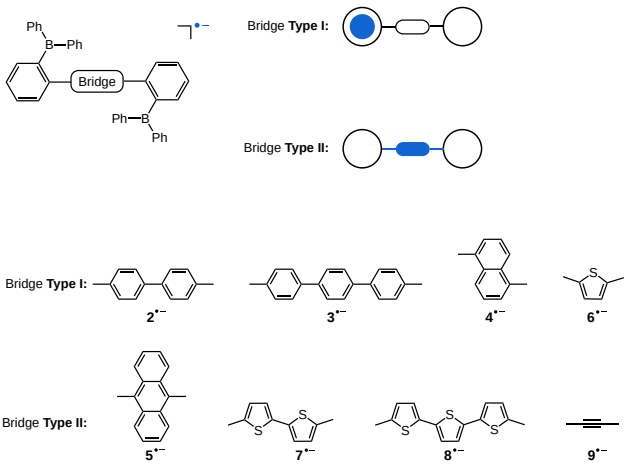


**Figure 5.** Diboryl monoradical anions with different bridge moieties. The blue shades show the distribution of the unpaired electron.

**Table 2.** Spin densities, Mulliken charges and dipole moments (in Debye) of the designed diboryl monoradical anions.

| | $S_{B1}$ | $S_{B2}$ | $Q_{B1}$ | $Q_{B2}$ | $\mu_x$ |
|---|---|---|---|---|---|
| **2**$^{\bullet-}$ | 0.602 | 0.003 | –0.226 | 0.035 | 22.5 |
| **3**$^{\bullet-}$ | 0.600 | 0.003 | –0.226 | 0.034 | 31.7 |
| **4**$^{\bullet-}$ | 0.604 | 0.012 | –0.224 | 0.042 | 16.7 |
| **6**$^{\bullet-}$ | 0.571 | 0.018 | –0.203 | 0.031 | 12.8 |
| **5**$^{\bullet-}$ | 0.028 | 0.028 | 0.058 | 0.058 | 0.0 |
| **7**$^{\bullet-}$ | 0.103 | 0.103 | –0.011 | –0.011 | 0.0 |
| **8**$^{\bullet-}$ | 0.000 | 0.074 | 0.048 | 0.000 | 4.1 |
| **9**$^{\bullet-}$ | 0.240 | 0.238 | –0.068 | –0.067 | 0.0 |

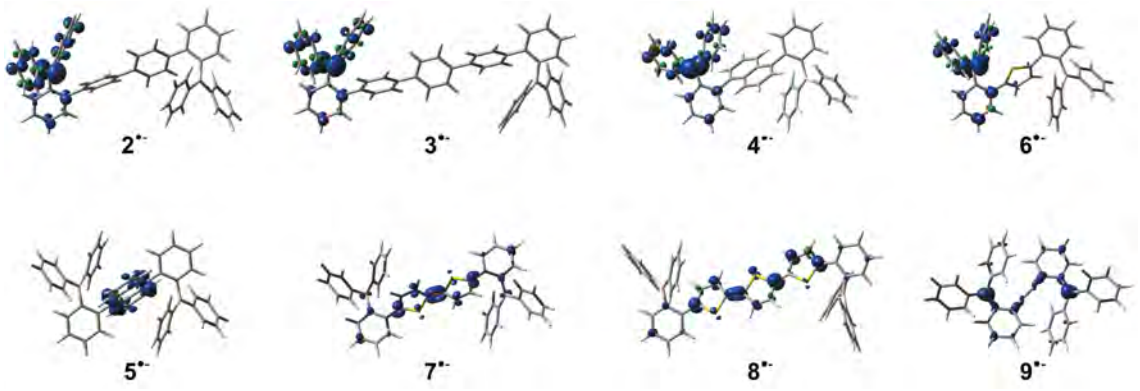


**Figure 6.** Spin density distributions for the designed diboryl monoradical anions.

### 3.4.2. Regiochemical Effect

Since the boron-$Ph_2$ groups in the above diboryl compounds are *ortho*-substituted to the two peripheral benzenes, it would be of interest to investigate their *meta*- and *para*-isomers. For the *meta*-isomer **1-*m*$^{\bullet-}$**, similar charge localization on one boron atom was observed (Figure 7) with a higher spin density (0.620) than **1**$^{\bullet-}$ (0.567). In contrast, the *para*-isomer **1-*p*$^{\bullet-}$** exhibits a delocalized charge distribution (Figure 7) mainly over boron atoms (0.203) and the transverse bonds of the central triphenyl moiety (0.360). By comparing their geometries (Figure S7), we found **1-*p*$^{\bullet-}$** was symmetrical and more like a quinonoid structure with a larger bond length alternation (BLA ~ 0.04 Å) of the central triphenyl group, as well as a longer boron-carbon$_{bridge}$ bond length (1.531 Å). While **1**$^{\bullet-}$ and **1-*m*$^{\bullet-}$** were unsymmetrical with a benzenoid central triphenyl group (BLA ~ 0.01 Å). The results for isomers of **2**$^{\bullet-}$ – **9**$^{\bullet-}$ are shown in Tables S4-S5 and Figures S8-S9. It is evident that all the isomers of **2**$^{\bullet-}$, **3**$^{\bullet-}$ and **4**$^{\bullet-}$ display charge distribution on one side of the molecule, while the *para*-isomers of the rest exhibit delocalized spin density distribution mostly over the spacer and boron atoms. Except **5**$^{\bullet-}$ and **8**$^{\bullet-}$, all the other *meta*-isomers show an uneven charge distribution. Therefore, candidate molecules with *meta*-substitution of the charge carrying unit are considered as the most promising when designing such kind of MQCA. The charge delocalization feature of the *para*-isomers, although not desirable for MQCA operation, may lead to optoelectronic properties if considerable overlap of the vacant boron p-orbital with the π-linker is present. Thus we conducted a rather preliminary exploration on the frontier molecular orbitals of the neutral compounds of the *para*-isomers (**1-*p*** – **9-*p***). Similar to many other triarylboranes,[41,42] an evident p-π* conjugation was observed in the LUMO delocalized over the whole molecule (Figure S10a), while the HOMO exhibits a major distribution on the π-conjugated bridge. So these compounds may probably be useful in the development of optoelectronic materials, which needs experimental verification in the future.

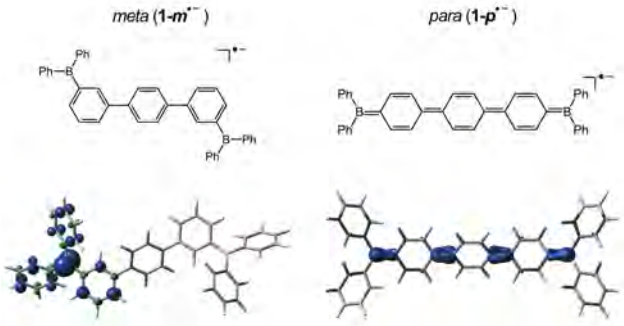


**Figure 7.** Spin density distributions for the *meta*- and *para*-isomers of $\mathbf{1}^{\bullet-}$.

## 4. CONCLUSIONS

Based on diboryl monoradical anions, a series of MQCA candidates have been proposed. DFT calculations show that the unpaired electron can be localized on either boron center, resulting in bistable charge configurations that can be switched either by an external electric field or by point charge drivers. With a dimer model, we demonstrated that the signal transmission can be realized via intermolecular Coulomb interaction. The study on bridge and regiochemical effects indicates *meta*-substitution of the charge carrying units connected by certain types of π-linkers as the optimal choice in the design of π-conjugated spacer linked diboryl MQCA candidates, which provides insightful guidance to experimental work. In addition, the neutral *para*-substituted diboryl compounds may have potential optoelectronic applications due to the presence of p-π* conjugation. It is worth noting that in laboratory synthesis, bulky substituents such as Mes need to be adopted to protect the boron radical centers and achieve better stability. Furthermore, as these candidates are radical anions, counterions are required to maintain charge neutrality of the system, which may perturb the local electric field and thus influence information transmission. This can be circumvented either by choosing appropriate counterions or by using neutral zwitterionic complexes. Future work on counterion effects and preparation of stable diboryl monoradical anions is under way.

**Supporting Information:**

Calculations of $E_{1/2}^{\mathrm{Red}}$ and $E_{\mathrm{d}}$; Spin densities, Mulliken charges and dipole moments (Tables S1-S5); Geometries (S1, S2, S7); Spin density distributions (S3-S6, S8, S9); Frontier molecular orbitals (S10)

## AUTHOR INFORMATION


### Corresponding Author

*E-mail: boxb@lzu.edu.cn (X.P.).

*E-mail: majing@nju.edu.cn (J.M.).

*E-mail: hyu@uow.edu.au (H.Y.).

### ORCID

Xingyong Wang: 0000-0002-6047-8722

Xiaobo Pan: 0000-0002-5757-2339

Jing Ma: 0000-0001-5848-9775

Haibo Yu: 0000-0002-1099-2803


### Notes

The authors declare no competing financial interest.

## ACKNOWLEDGEMENTS


This work has been supported by the Vice-Chancellor's Postdoctoral Research Fellowship Funding of the University of Wollongong (X.W.) and the computational resources provided by NCI's National Computational Merit Allocation Scheme. H.Y. is the recipient of an Australian Research Council Future Fellowship (Project number FT110100034). This research was in part supported under the Australian Research Council's Discovery Projects funding scheme (project number DP170101773, H.Y.). We also acknowledge the support from the Natural Science Foundation of Gansu Province (No. 1506RJZA213, X.P.) and the National Natural Science Foundation of China (No. 21673111, J.M.)

**REFERENCES**


(1) Orlov, A. O.; Amlani, I.; Bernstein, G. H.; Lent, C. S.; Snider, G. L., Realization of a Functional Cell for Quantum-Dot Cellular Automata. *Science* **1997**, *277*, 928-930.

(2) Lent, C. S.; Tougaw, P. D.; Porod, W.; Bernstein, G. H., Quantum Cellular Automata. *Nanotechnology* **1993**, *4*, 49-57.

(3) Tougaw, P. D.; Lent, C. S., Logical Devices Implemented Using Quantum Cellular Automata. *J. Appl. Phys.* **1994**, *75*, 1818-1825.

(4) Lent, C. S.; Tougaw, P. D., A Device Architecture for Computing with Quantum Dots. *Proc. IEEE* **1997**, *85*, 541-557.

(5) Amlani, I.; Orlov, A. O.; Toth, G.; Bernstein, G. H.; Lent, C. S.; Snider, G. L., Digital Logic Gate Using Quantum-Dot Cellular Automata. *Science* **1999**, *284*, 289-291.

(6) Cowburn, R. P.; Welland, M. E., Room Temperature Magnetic Quantum Cellular Automata. *Science* **2000**, *287*, 1466-1468.

(7) Imre, A.; Csaba, G.; Ji, L.; Orlov, A.; Bernstein, G. H.; Porod, W., Majority Logic Gate for Magnetic Quantum-Dot Cellular Automata. *Science* **2006**, *311*, 205-208.

(8) Haider, M. B.; Pitters, J. L.; DiLabio, G. A.; Livadaru, L.; Mutus, J. Y.; Wolkow, R. A., Controlled Coupling and Occupation of Silicon Atomic Quantum Dots at Room Temperature. *Phys. Rev. Lett.* **2009**, *102*, 046805.

(9) Lent, C. S., Bypassing the Transistor Paradigm. *Science* **2000**, *288*, 1597-1599.

(10) Hennessy, K.; Lent, C. S., Clocking of Molecular Quantum-Dot Cellular Automata. *J. Vac. Sci. Technol., B* **2001**, *19*, 1752-1755.

(11) Hush, N., Molecular Electronics: Cool Computing. *Nat. Mater.* **2003**, *2*, 134-135.

(12) Lent, C. S.; Isaksen, B.; Lieberman, M., Molecular Quantum-Dot Cellular Automata. *J. Am. Chem. Soc.* **2003**, *125*, 1056-1063.

(13) Lu, Y.; Liu, M.; Lent, C., Molecular Quantum-Dot Cellular Automata: From Molecular Structure to Circuit Dynamics. *J. Appl. Phys.* **2007**, *102*, 034311.

(14) Lu, Y.; Lent, C., A Metric for Characterizing the Bistability of Molecular Quantum-Dot Cellular Automata. *Nanotechnology* **2008**, *19*, 155703.

(15) Lu, Y.; Lent, C. S., Field-Induced Electron Localization: Molecular Quantum-Dot Cellular Automata and the Relevance of Robin–Day Classification. *Chem. Phys. Lett.* **2015**, *633*, 52-57.

(16) Jiao, J.; Long, G. J.; Grandjean, F.; Beatty, A. M.; Fehlner, T. P., Building Blocks for the Molecular Expression of Quantum Cellular Automata. Isolation and Characterization of a Covalently Bonded Square Array of Two Ferrocenium and Two Ferrocene Complexes. *J. Am. Chem. Soc.* **2003**, *125*, 7522-7523.

(17) Li, Z.; Beatty, A. M.; Fehlner, T. P., Molecular QCA Cells. 1. Structure and Functionalization of an Unsymmetrical Dinuclear Mixed-Valence Complex for Surface Binding. *Inorg. Chem.* **2003**, *42*, 5707-5714.

(18) Li, Z.; Fehlner, T. P., Molecular QCA Cells. 2. Characterization of an Unsymmetrical Dinuclear Mixed-Valence Complex Bound to a Au Surface by an Organic Linker. *Inorg. Chem.* **2003**, *42*, 5715-5721.

(19) Qi, H.; Sharma, S.; Li, Z.; Snider, G. L.; Orlov, A. O.; Lent, C. S.; Fehlner, T. P., Molecular Quantum Cellular Automata Cells. Electric Field Driven Switching of a Silicon Surface Bound Array of Vertically Oriented Two-Dot Molecular Quantum Cellular Automata. *J. Am. Chem. Soc.* **2003**, *125*, 15250-15259.

(20) Braun-Sand, S. B.; Wiest, O., Theoretical Studies of Mixed-Valence Transition Metal Complexes for Molecular Computing. *J. Phys. Chem. A* **2003**, *107*, 285-291.

(21) Braun-Sand, S. B.; Wiest, O., Biasing Mixed-Valence Transition Metal Complexes in Search of Bistable Complexes for Molecular Computing. *J. Phys. Chem. B* **2003**, *107*, 9624-9628.

(22) Qi, H.; Gupta, A.; Noll, B. C.; Snider, G. L.; Lu, Y.; Lent, C.; Fehlner, T. P., Dependence of Field Switched Ordered Arrays of Dinuclear Mixed-Valence Complexes on the Distance between the Redox Centers and the Size of the Counterions. *J. Am. Chem. Soc.* **2005**, *127*, 15218-15227.

(23) Jiao, J.; Long, G. J.; Rebbouh, L.; Grandjean, F.; Beatty, A. M.; Fehlner, T. P., Properties of a Mixed-Valence $(Fe^{II})_2(Fe^{III})_2$ Square Cell for Utilization in the Quantum Cellular Automata Paradigm for Molecular Electronics. *J. Am. Chem. Soc.* **2005**, *127*, 17819-17831.

(24) Lu, Y.; Lent, C. S., Theoretical Study of Molecular Quantum-Dot Cellular Automata. *J. Comput. Electron.* **2005**, *4*, 115-118.

(25) Zhao, Y.; Guo, D.; Liu, Y.; He, C.; Duan, C., A Mixed-Valence $(Fe^{II})_2(Fe^{III})_2$ Square for Molecular Expression of Quantum Cellular Automata. *Chem. Commun.* **2008**, 5725-5727.

(26) Nemykin, V. N.; Rohde, G. T.; Barrett, C. D.; Hadt, R. G.; Bizzarri, C.; Galloni, P.; Floris, B.; Nowik, I.; Herber, R. H.; Marrani, A. G., et al., Electron-Transfer Processes in Metal-Free Tetraferrocenylporphyrin. Understanding Internal Interactions to Access Mixed-Valence States Potentially Useful for Quantum Cellular Automata. *J. Am. Chem. Soc.* **2009**, *131*, 14969-14978.

(27) Schneider, B.; Demeshko, S.; Dechert, S.; Meyer, F., A Double-Switching Multistable $Fe_4$ Grid Complex with Stepwise Spin-Crossover and Redox Transitions. *Angew. Chem. Int. Ed.* **2010**, *49*, 9274-9277.

(28) Lu, Y.; Quardokus, R.; Lent, C. S.; Justaud, F.; Lapinte, C.; Kandel, S. A., Charge Localization in Isolated Mixed-Valence Complexes: An Stm and Theoretical Study. *J. Am. Chem. Soc.* **2010**, *132*, 13519-13524.

(29) Guo, S.; Kandel, S. A., Scanning Tunneling Microscopy of Mixed Valence Dinuclear Organometallic Cations and Counterions on Au(111). *J. Phys. Chem. Lett.* **2010**, *1*, 420-424.

(30) Tsukerblat, B.; Palii, A.; Clemente-Juan, J. M.; Coronado, E., Mixed-Valence Molecular Four-Dot Unit for Quantum Cellular Automata: Vibronic Self-Trapping and Cell-Cell Response. *J. Chem. Phys.* **2015**, *143*, 134307.

(31) Clemente-Juan, J. M.; Palii, A.; Coronado, E.; Tsukerblat, B., Mixed-Valence Molecular Unit for Quantum Cellular Automata: Beyond the Born-Oppenheimer Paradigm through the Symmetry-Assisted Vibronic Approach. *J. Chem. Theory. Comput.* **2016**, *12*, 3545-3560.

(32) Palii, A.; Tsukerblat, B.; Clemente-Juan, J. M.; Coronado, E., Spin Switching in Molecular Quantum Cellular Automata Based on Mixed-Valence Tetrameric Units. *J. Phys. Chem. C* **2016**, *120*, 16994-17005.

(33) Erickson, N. R.; Holstrom, C. D.; Rhoda, H. M.; Rohde, G. T.; Zatsikha, Y. V.; Galloni, P.; Nemykin, V. N., Tuning Electron-Transfer Properties in 5,10,15,20-Tetra(1'-Hexanoylferrocenyl)Porphyrins as Prospective Systems for Quantum Cellular Automata and Platforms for Four-Bit Information Storage. *Inorg. Chem.* **2017**, *56*, 4717-4728.

(34) Schneider, B.; Demeshko, S.; Neudeck, S.; Dechert, S.; Meyer, F., Mixed-Spin [2 × 2] $Fe_4$ Grid Complex Optimized for Quantum Cellular Automata. *Inorg. Chem.* **2013**, *52*, 13230-13237.

(35) Lei, X.; Wolf, E. E.; Fehlner, T. P., Clusters as Ligands – Large Assemblies of Transition Metal Clusters. *Eur. J. Inorg. Chem.* **1998**, *1998*, 1835-1846.

(36) Lu, Y.; Lent, C., Self-Doping of Molecular Quantum-Dot Cellular Automata: Mixed Valence Zwitterions. *Phys. Chem. Chem. Phys.* **2011**, *13*, 14928-14936.

(37) Lu, Y.; Lent, C. S., Counterion-Free Molecular Quantum-Dot Cellular Automata Using Mixed Valence Zwitterions – a Double-Dot Derivative of the [*closo*-1-$CB_9H_{10}$]$^-$ Cluster. *Chem. Phys. Lett.* **2013**, *582*, 86-89.

(38) Wang, X.; Ma, J., Electron Switch in the Double-Cage Fluorinated Fullerene Anions, $e^-$@$C_{20}F_{18}(XH)_2C_{20}F_{18}$ (X = N, B): New Candidates for Molecular Quantum-Dot Cellular Automata. *Phys. Chem. Chem. Phys.* **2011**, *13*, 16134-16137.

(39) Wang, X.; Chen, S.; Wen, J.; Ma, J., Exploring the Possibility of Noncovalently Surface Bound Molecular Quantum-Dot Cellular Automata: Theoretical Simulations of Deposition of Double-Cage Fluorinated Fullerenes on Ag(100) Surface. *J. Phys. Chem. C* **2013**, *117*, 1308-1314.

(40) Yu, L.; Li, Y.; Wang, X.; Wang, X.; Zhou, P.; Jiang, S.; Pan, X., Consecutive Reduction, Radical-Cyclization, and Oxidative-Dehydrogenation Reaction of Ortho-Substituted Diboryl Compounds. *Chem. Commun.* **2017**, *53*, 9737-9740.

(41) Jäkle, F, Advances in the Synthesis of Organoborane Polymers for Optical, Electronic, and Sensory Applications. *Chem. Rev.* **2010**, *110*, 3985-4022.

(42) Ji, L.; Griesbeck, S.; Marder, T. B., Recent Developments in and Perspectives on Three-Coordinate Boron Materials: A Bright Future. *Chem. Sci.* **2017**, *8*, 846-863.

(43) Wade, C. R.; Broomsgrove, A. E. J.; Aldridge, S.; Gabbaï, F. P., Fluoride Ion Complexation and Sensing Using Organoboron Compounds. *Chem. Rev.* **2010**, *110*, 3958-3984.

(44) Schickedanz, K.; Radtke, J.; Bolte, M.; Lerner, H.-W.; Wagner, M., Facile Route to Quadruply Annulated Borepins. *J. Am. Chem. Soc.* **2017**, *139*, 2842-2851.

(45) Frisch, M. J. G.; Trucks, W.; Schlegel, H. B.; Scuseria, G. E.; Robb, M. A.; Cheeseman, J. R.; Scalmani, G.; Barone, V.; Mennucci, B.; Petersson, G. A.; et al. *Gaussian 09*, Revision D.01; Gaussian, Inc., Wallingford CT, 2013. See SI for full citation.

(46) Su, Y.; Wang, X.; Zheng, X.; Zhang, Z.; Song, Y.; Sui, Y.; Li, Y.; Wang, X., Tuning Ground States of Bis(Triarylamine) Dications: From a Closed-Shell Singlet to a Diradicaloid with an Excited Triplet State. *Angew. Chem. Int. Ed.* **2014**, *53*, 2857-2861.

(47) Su, Y.; Wang, X.; Li, Y.; Song, Y.; Sui, Y.; Wang, X., Nitrogen Analogues of Thiele's Hydrocarbon. *Angew. Chem. Int. Ed.* **2015**, *54*, 1634-1637.

(48) Wang, X.; Zhang, Z.; Song, Y.; Su, Y.; Wang, X., Bis(Phenothiazine)Arene Diradicaloids: Isolation, Characterization and Crystal Structures. *Chem. Commun.* **2015**, *51*, 11822-11825.

**Table of Contents Graphic:**